Supporting Information

Cost-Effective Conversion of "Stones" into High-Performance Capacitor Carbon through Solid-Solid Inorganic Chemical Reaction

Yongfeng Bu[a], Shihao Wang[a], Yuman Li[a], Shengda Tang[b], Qin Kang[a], Zhaomin Zhu[a], Hui Li[b], Li Pan[b], Hongyu Liang[b,]*

[a]*Institute for Energy Research, Jiangsu University, Zhenjiang, 212013, China*

[b]*Institute of Advanced Manufacturing and Modern Equipment Technology, School of Mechanical Engineering, Jiangsu University, Zhenjiang, 212013, China*

**E-mail address*: hyliang@ujs.edu.cn

Contents:

Fig. S7 Cycling stability and Coulombic efficiency of YP50F in KOH/H_2O electrolyte.

Table S1 Comparison of TC with carbon derived from CaC_2, $CaCO_3$ and others on parameters and capacitance properties.

Table S2 Collection for the R_s, R_{ct}, R_w, and R_{ESR} of TC and YP50F in aqueous and organic electrolytes.

Table S3 Cost evaluation for the preparation of 1 kg of TC.

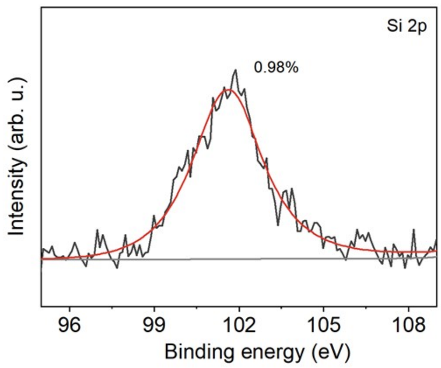

Fig. S1 The corresponding fine spectra of Si 2p of TC.

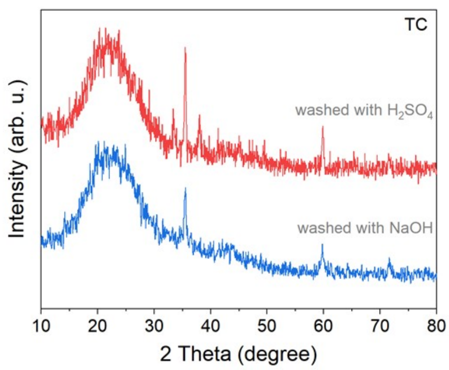

Fig. S2 XRD patterns of TC treated by 5 mol L^{-1} H_2SO_4 and 10 mol L^{-1} NaOH solutions, respectively.

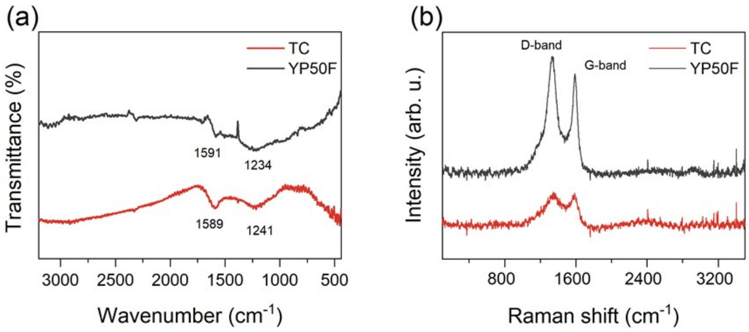

Fig. S3 Component characterization of TC. a) FTIR analysis; b) Raman spectra. The data of YP50F are provided for comparison.

FT-IR spectral data of TC show two major adsorption bands at 1241 cm^{-1} and 1589 cm^{-1}, corresponding to the backbone vibration of C=C and the stretching vibration of C-O-C, respectively. The presence of oxygen-containing groups on the surface of TC is demonstrated, which can improve the hydrophilicity of TC in aqueous/organic electrolytes. Typical D-peak (~1345 cm^{-1}) and G-peaks (~1586 cm^{-1}) can be observed, and the positions of the peaks approximately overlap with YP50F.

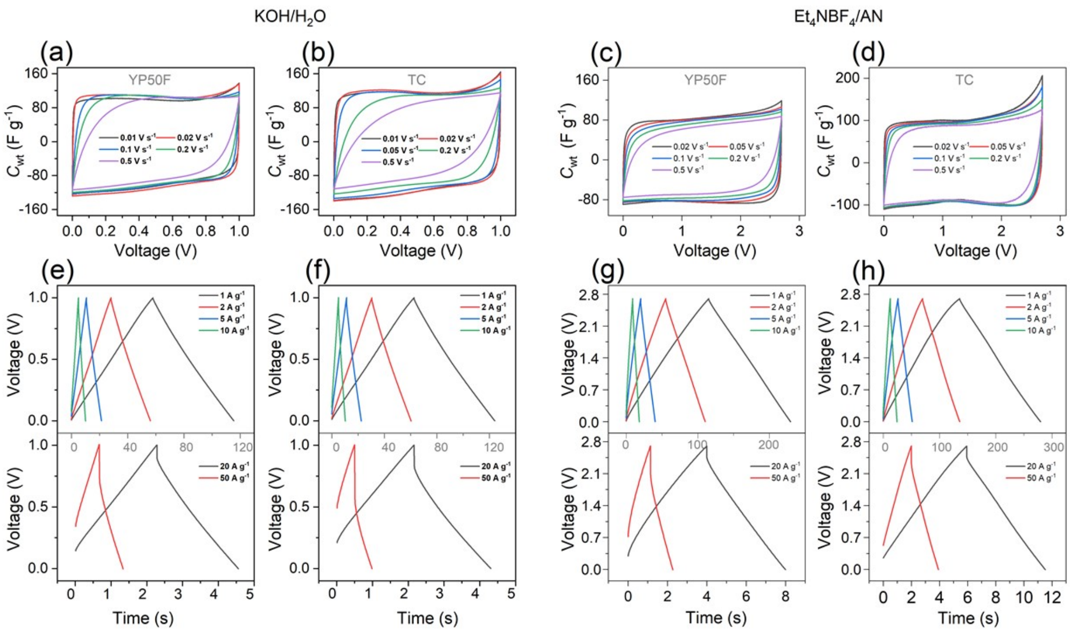

Fig. S4 Electrochemical performance of symmetrical SCs using TC as electrodes in aqueous and organic electrolytes, respectively. a, b) CV curves at 0.01-0.5 V s^{-1} in KOH/H_2O; c, d) CV curves at 0.02-0.5 V s^{-1} in Et_4NBF_4/AN; e, f) GCD curves at different current densities (i.e., 1-50 A g^{-1}) in KOH/H_2O, respectively; g, h) GCD curves at 1-50 A g^{-1} in Et_4NBF_4/AN. The data of YP50F are also provided for comparison.

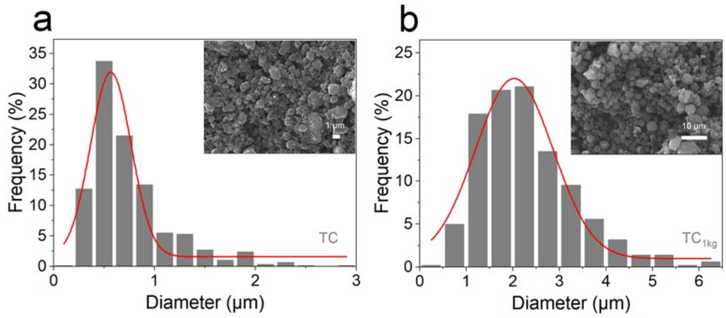

Fig. S5 Characterizations of average particle size distribution. a) TC; b) TC_{1kg}. The inset is the corresponding SEM image.

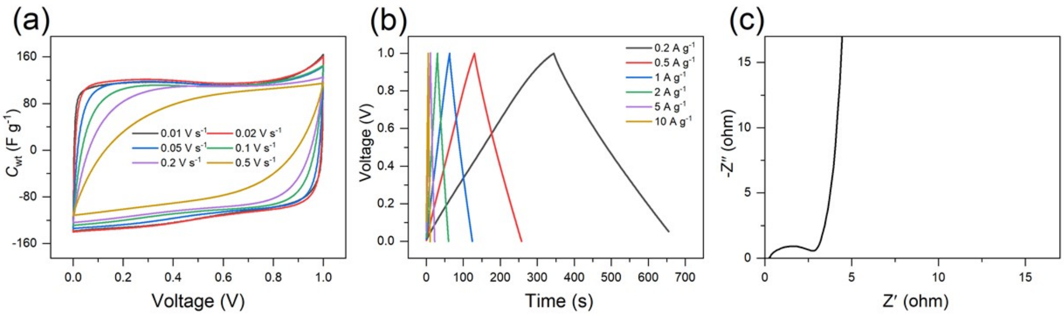

Fig. S6 Electrochemical performance of symmetrical SCs using TC_{1kg} as electrodes in 6.0 mol L^{-1} KOH/H_2O electrolyte. a) CV curves at 0.01-0.5 V s^{-1}); b) GCD curves at 0.2-10 A g^{-1}); c) Nyquist plots.

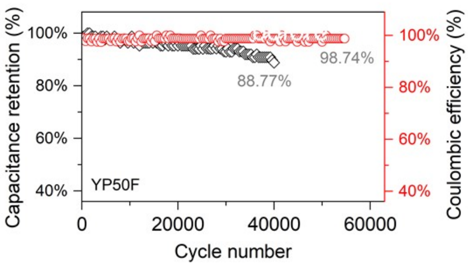

Fig. S7 Cycling stability and Coulombic efficiency of YP50F at 5 A g^{-1} in 6.0 mol L^{-1} KOH/H_2O electrolyte.

Table S1 Comparison of TC with carbon derived from CaC_2, $CaCO_3$ and others on parameters and capacitance properties.

Various carbon	Samples	SSA	Electrolyte	Current density /Scan rate	C_{wt} (F g^{-1})	Note	Refs.
CaC_2 -derived carbon	TC	1090	6M KOH	1 A g^{-1}	127	/	This study
	CDC-Zn	191	6M KOH	1 mV s^{-1}	105	/	[1]
	OACM	687	6M KOH	0.15 A g^{-1}	121	/	[2]
	CCDPC	525	1M KOH	0.5 A g^{-1}	116	/	[3]
	CCDC	612	6M KOH	10 mV s^{-1}	108	/	[4]
	CaC_2-CDC	800	6M KOH	10 mV s^{-1}	126	/	[5]
$CaCO_3$ -derived carbon	Sample (850℃)	325	/	5 mV s^{-1}	84	/	[6]
	Carbon-DC	652	6M KOH	1 A g^{-1}	176	/	[7]
	3-6-800	544	/	100 mV s^{-1}	190	/	[8]
	NPC4	1133	1M H_2SO_4	0.5 A g^{-1}	162	5.9 at. % N-doped	[9]
CO_2 converted carbon	SHSG-8	709	1 M $EMIMBF_4$	2 A g^{-1}	172	/	[10]
	TC-1	1020	6M KOH	1 A g^{-1}	140	/	[11]
	CPC1_700	1262	6M KOH	1 A g^{-1}	270	0.45 at. % B-doped	[12]
Biomass -derived carbon	PGCS-1-1100	540	6M KOH	1 A g^{-1}	213	/	[13]
	FC-0-8	479	6M KOH	1 A g^{-1}	84.3	/	[14]
	CNS/$CF_{0.15}$	1068	6M KOH	0.5 A g^{-1}	355	/	[15]
MOF -derived carbon	NHCSF-3	816	6M KOH	1 A g^{-1}	254	20 at. % N-doped	[16]
	HPCNFs-N	418	2M H_2SO_4	5 A g^{-1}	264	/	[17]
	MIL-101-NH_2	2987	1M H_2SO_4	0.1 A g^{-1}	272	9.6 at. % N-doped	[18]
Carbon derived from others	MWCNT	130-410	6M KOH	10 mV s^{-1}	80-135	/	[19]
	GH-H	951	5M KOH	1 A g^{-1}	220	C/N= 36.7	[20]
	HGF-EC	2630	1M $EMIMIBF_4$	1 A g^{-1}	298	/	[21]
	N/P-TRGO	152	6M KOH	0.1 A g^{-1}	165	2.9 at. % N-doped + 4.3 at. % P-doped	[22]
	GNS/CB-2	586	6M KOH	10 mV s^{-1}	175	/	[23]

Table S2 Collection for the R_s, R_{ct}, R_w, and R_{ESR} of TC and YP50F in aqueous and organic electrolytes.

Samples	R_s (Ω)	R_{ct} (Ω)	R_w (Ω)	R_{ESR} (Ω)
TC (KOH/H_2O)	0.27	0.67	1.88	2.82
TC_{1kg} (KOH/H_2O)	0.28	1.74	3.18	5.20
YP50F (KOH/H_2O)	0.21	2.44	2.82	5.47
TC (Et_4NBF_4/AN)	1.94	0.64	1.72	4.30
TC_{1kg} (Et_4NBF_4/AN)	1.72	0.69	3.61	6.03
YP50F (Et_4NBF_4/AN)	2.74	2.21	8.14	13.09

Table S3 Cost evaluation for the preparation of 1 kg of TC.

	Materials	Consumption	Price (RMB)	Total (RMB)
Raw materials	CaC_2	1.3 kg	2.7	4
	$CaCO_3$	1 kg	0.5	
Energy	Ball milling	44 kWh	0.49	26.4
	Drying	10 kWh	0.49	
Auxiliary materials	HCl	25 kg	0.4	15.6
	N_2	1.25 L	4.5	

References

1. K. Zhang, S. Tao, X. Xu, H. Meng, Y. Lu and C. Li, Preparation of mesoporous carbon materials through mechanochemical reaction of calcium

carbide and transition metal chlorides, *Ind. Eng. Chem. Res.*, 2018, **57**, 6180-6188.

2. Y. Li, S. Li, X. Xu, J. Gu, X. He, H. Meng, Y. Lu and C. Li, Converting CO_2 into an oxygenated alkynyl carbon material with high electrochemical performance through a mechanochemical reaction with CaC_2, *ACS Sustainable Chem. Eng.*, 2021, **9**, 9221-9229.
3. J. Yang, Y. Chen, J. Peng, J. Zeng, G. Li, B. Chang, Y. Shen, X. Guo, G. Chen, X. Wang and L. Zheng, Green preparation and supercapacitive behaviors of calcium carbide derived porous carbon based on solvent free mechanochemical route, *J. Energy Storage*, 2022, **51**, 104473.
4. L. Zheng, Y. Wang, X. Wang, X. Wang, H. An and L. Yi, The effects of surface modification on the supercapacitive behaviors of carbon derived from calcium carbide, *J. Mater. Sci.*, 2010, **45**, 6030-6037.
5. C. Dai, X. Wang, Y. Wang, N. Li and J. Wei, Synthesis of nanostructured carbon by chlorination of calcium carbide at moderate temperatures and its performance evaluation, *Mater. Chem. Phys.*, 2008, **112**, 461-465.
6. R. Liu, S. Yao, Y. Shen, Y. Tian and Q. Zhang, Preparation of N doped layered porous carbon and its capacitive deionization performance, *Materials*, 2023, **16**, 1435.
7. Z. Xiao, Y. Zhu, H. Yi and X. Chen, A simple $CaCO_3$ assisted template carbonization method for producing nitrogen containing nanoporous carbon

spheres and its electrochemical improvement by the nitridation of azodicarbonamide, *Electrochim. Acta*, 2015, **155**, 93-102.

8. F. Shen, M. Qiu, Y. Hua and X. Qi, Dual functional templated methodology for the synthesis of hierarchical porous carbon for supercapacitor, *ChemistrySelect*, 2018, **3**, 586-591.

9. Z. Sun, W. Wang, J. Zhang, G. Wang, K. Wang, X. Liu, G. Ni and Y. Jiang, Nitrogen rich hierarchical porous carbon materials with interconnected channels for high stability supercapacitors, *New J. Chem.*, 2019, **43**, 1864-1873.

10. C. Li, X. Zhang, K. Wang, X. Sun, G. Liu, J. Li, H. Tian, J. Li and Y. Ma, Scalable self propagating high temperature synthesis of graphene for supercapacitors with superiorpower density and cyclic stability, *Adv. Mater.*, 2016, **29**, 1604690.

11. H. Liang, R. Shi, Y. Zhou, W. Jiang, T. Sun, Z. Zhang, L. Sun, J. Lian, H. Li and Y. Bu, Removing cost barriers to template carbon synthesis for high performance supercapacitors by establishing a zero emission chemical cycle from CO_2, *ACS Energy Lett.*, 2022, **7**, 4381-4388.

12. Y. K. Kim, J. H. Park and J. W. Lee, Facile nano templated CO_2 conversion into highly interconnected hierarchical porous carbon for high performance supercapacitor electrodes, *Carbon*, 2018, **126**, 215-224.

13. L. Wang, G. Mu, C. Tian, L. Sun, W. Zhou, P. Yu, J. Yin and H. Fu, Porous graphitic carbon nanosheets derived from cornstalk biomass for advanced supercapacitors, *ChemSusChem*, 2013, **6**, 880-889.

14. A. Guo, X. Zhang, B. Shao, S. Sang and X. Yang, Catalytic graphitization assisted synthesis of Fe_3C/Fe/graphitic carbon with advanced pseudocapacitance, *RSC Adv.*, 2022, **12**, 7935-7940.

15. X. Zhang, B. Liu, X. Yan, X. Zhao, Y. Zhang, Y. Wei and Q. Cao, Design and structure optimization of 3D porous graphitic carbon nanosheets for high performance supercapacitor, *Microporous Mesoporous Mater.*, 2020, **309**, 11058.

16. Z. Li, H. Mi, L. Liu, Z. Bai, J. Zhang, Q. Zhang and J. Qiu, Nano sized ZIF-8 anchored polyelectrolyte decorated silica for nitrogen rich hollow carbon shell frameworks toward alkaline and neutral supercapacitors, *Carbon*, 2018, **136**, 176-186.

17. L. F. Chen, Y. Lu, L. Yu and X. W. Lou, Designed formation of hollow particle based nitrogen doped carbon nanofibers for high performance supercapacitors, *Energy Environ. Sci.*, 2017, **10**, 1777-1783.

18. Q. L. Zhu, P. Pachfule, P. Strubel, Z. Li, R. Zou, Z. Liu, S. Kaskel and Q. Xu, Fabrication of nitrogen and sulfur Co-doped hollow cellular carbon nanocapsules as efficient electrode materials for energy storage, *Energy Storage Mater.*, 2018, **13**, 72-79.

19. E. Frackowiak, K. Metenier, V. Bertagna and F. Beguin, Supercapacitor electrodes from multiwalled carbon nanotubes, *Appl. Phys. Lett.*, 2000, **77**, 2421-2423.

20. L. Zhang and G. Shi, Preparation of highly conductive graphene hydrogels for fabricating supercapacitors with high rate capability, *J. Phys. Chem. C*, 2011, **115**, 17206-17212.

21. Y. Xu, Z. Lin, X. Zhong, X. Huang, N. O. Weiss, Y. Huang and X. Duan, Holey graphene frameworks for highly efficient capacitive energy storage, *Nat. Commun.*, 2014, **5**, 4554.

22. C. Wang, Y. Zhou, L. Sun, Q. Zhao, X. Zhang, P. Wan and J. Qiu, N/P-Co doped thermally reduced graphene for high performance supercapacitor applications, *J. Phys. Chem. C*, 2013, **117**, 14912-14919.

23. J. Yan, T. Wei, B. Shao, F. Ma, Z. Fan, M. Zhang, C. Zheng, Y. Shang, W. Qian and F. Wei, Electrochemical properties of graphene nanosheet/carbon black composites as electrodes for supercapacitors, *Carbon*, 2010, **48**, 1731-1737.